# Case Study of GIS Application in Analysing Urban Heating Island Phenomena in Tropical Climate Country

IOP Conf. Series: Materials Science and Engineering **661** (2019) 012090 doi:10.1088/1757-899X/661/1/012090

# Case Study of GIS Application in Analysing Urban Heating Island Phenomena in Tropical Climate Country

**Minh Tuan Le[1], Thi Anh Tuyet Cao[2], Nguyen Anh Quan Tran[3], Shukurov Ilkhomhon Sadriavich[1], Thi Khanh Phuong Nguyen[1], Thi Kim Cuong Le[1]**

[1] Moscow State university of Civil Engineering, Yaroslavskoye Shosse, 26, Moscow, 129337, Russia
[2] Moscow State university of Geodesy and Cartography, Gorokhovsky pereulok, 4, Moscow, 105064, Russia
[3] Peter the Great St. Petersburg Polytechnic University, Politekhnicheskaya Ulitsa, 29, Sankt-Petersburg, 195251

architect290587@gmail.com

**Abstract.** This study indicates Urban Heat Island phenomena (UHI) in districts belonged to Hanoi city located in tropical climate region. The analysis based on assessment's comparison by applying remote sensing technology. The data captured in partly cloudy days and at night time by satellite Landsat 5, 7, 8 and is converted subsequently into Land Surface Temperature (LST) range maps. Spatial patterns of UHIs in Hanoi city were examined over the daytime and seasonal variations. Gaussian approximation algorithm is used to quantify spatial extents and measure magnitude for each individual UHIs. Consequently, to determine the relationship of UHIs with surface properties, UHI patterns were analyzed in association with urban vegetation covers and surface energy fluxes derived from high-resolution Landsat 5, 7, 8 data. A general picture of UHI phenomena in Hanoi city in this study and analyzed results, by applying integrating satellite high-resolution thermal data with land-surface modelling and meso-scale climatic modelling, to further address the impacts of urbanization in local climate cities, propose a framework for sustainable urban planning design in the future.

## 1. Introduction

The temperature of the land surface plays an important role in the physical processes occurring in the soil and the atmosphere, which is one of the important factors that directly affect the environment and human life [1,10]. Nevertheless, to determine the surface temperature of a large area, by using the meteorological monitoring station, should be placed on land surface in large quantities and operate for long periods of time, the purpose is to provide information about the surface accurately [2,11]. While the rapid process of urbanization in Vietnam is now gradually concentrating on the vegetation cover, which leads to an increase in surface temperature, contributing significantly to global warming, causing natural disasters.

The United States is one of the leading countries in the study of the earth's surface according to satellite imagery, usually Landsat satellites, which started with Landsat-1, which was successfully launched in 1972

[3,12]. There are 8 generations of Landsat, but only Landsat is active - 7 and 8 [13,14]. Starting with the Landsat-4 and 5 generations, in which the TM (Thematic Mapper) sensor captured thermal radiation energy, and the Landsat-7 generation in addition to the pretty MMS (multispectral scanner), it provides a multispectral image that it still carries [15]. According to the ETM + (Enhanced Thematic Mapper +) sensor, it is also possible to capture the radiant heat energy of objects on natural surfaces and to get a thermal image with a fairly high resolution. [4,5] Using this data source, you can determine the temperature of any area on the earth [16, 17, 18].

After the expansion to the administrative border, the capital of Hanoi increased to 30 administrative units since 2008, including 12 districts and 17 districts with an area of 3,344.7 km2, and the population increased to almost 7 million people. In addition, immigrants occupy a large number, thus the development of infrastructure and housing is expanding, causing the phenomenon of "Urban Heating Island" in urban areas (the surface of urban areas is higher than the surrounding areas), [6]. The Landsat-5 TM and Landsat-8 OLI /TIRS image data (land scanner, thermal infrared sensor) will become an important and effective source of data for calculating surface temperature and determining the condition of urban land, thereby finding a correlation between surface temperature and surface coating. [7, 8, 19]

## 2. Used Method

Firstly it must be determined the current surface condition of the coating. The accredited classification method is a classification form in which classification criteria are established based on sample areas and using decision rules based on appropriate algorithms for labelling pixels corresponding to each specific coverage. The mathematics chosen for execution is a maximum probability algorithm [9,20].

$$g_l(x) = \ln p(\omega_i) - \frac{1}{2}\ln(x - m_i)^T \sum_i - l(x - m_i) \quad (1)$$

where: i objects of classification; x: number of universal channels; p ( $\omega_i$ ): the probability value occurs when the object $\omega_i$ is similar to other objects;

$|\omega_i|$: The covariance matrix of the object $\omega_i$ ; $\sum_i -1$ Inverse matrix of object $\omega_i$ ; $m_i$ change the values of the vector.

This is the correct classification, but it takes a lot of time to calculate and depends on the normal distribution of data. Include the following steps:

- Determine the types of land to use to build the key interpretation of the image.
- The choice of the properties of the spectra and structure for the separation of objects from each other.
- Select the image area to select it directly on the image, then decide to sort the results.
- The evaluation of the accuracy of the sample file compares the differences of each sample with other samples.
- To assess the accuracy of image classification based on the Kappa index (K), this index is in the range from 0 to 1 and indicates a proportional decrease in the error made in the complete classification randomly.

$$K = \left[ N\sum_{i=1}^{r} x_{ii} - \sum_{i=1}^{r} (x_{i+}...x_{+1}) \right] / \left[ N^2 - \sum_{i=1}^{r} (x_{i+}...x_{+1}) \right] \quad (2)$$

where:

N: total number of sampling points;
r: number of class objects
xii: the number of field points is correct in the first grade;
xi +: common point of the field of the class i of the sample;
x + i: the total number of field points of the next *i* class classification.

**3. Results**

Determination of the current state of surface coatings in 2007, 2012 and 2017. The remote sensing data used in the project includes 3 Landsat multispectral satellite images covering the study area for 2007, 2012 and 2017, all of which are medium resolution images. Remote sensing data used in this topic includes 3 Landsat satellite imagery covering three survey locations in 2007, 2012 and 2017.

In addition to satellite images, the following data is also used in the subject:

- Topographical map of the district of Hanoi
- The necessary data on the area of the city of Hanoi (geographical location, natural conditions, population, socio-economic situation ...).
- Identification of the classification system is the first important task when applying remote sensing to build a cover state map. The categorical glossary system should be consistent with the ability to provide information to remote sensing data. Configuring annotations is based not only on objects visible in the image, but also on many other factors: image resolution, nature of the season, time spent and knowledge of the field.
- Image display: There are two display modes consists of grayscale (black and white display) and RGB colour (combination of colours).
- RGB colour: a combination of colours, with three primary colours: red (Red), blue (Blue) and green (Green).

In general, the accuracy of the image fragmentation results is based on the correct choice of the fragmentation algorithm, the choice of proportional parameters and the choice of weights for shapes, colours and density (compactness), smoothness. After running the test and verifying the results of image fragmentation and finally choosing the most appropriate parameters to use for fragmentation of the image, Landsat TM in 2007 as follows: the ratio of parameters is 10, shape 0.1 and density 0.5, colour 0.9, smoothness 0.5 gives the best results of image fragmentation. The following is the result of the dissertation photo fragmentation process.

With an existing source of data and local knowledge, students can develop a glossary as follows table 1. The results of satellite image processing by remote sensing show that over 15 years, from 2007 to 2017, the area of urban land (building land) has increased 2.16 times (table 2 and figure 2). In figure 1, an area of 12 urban districts thrive in the direction of spreading from the central region and concentrating on all sides, especially along the main roads in the central border.

In general, the results (figure 2) show a plot of land for development in terms of scale and percentage of soil by type of use from 2007 to 2017. The rate of growth of building land is quickly in line with the context of rapid urbanization in the city Hanoi. In particular, the share of urban green space for the period 2007–2017 decreased from 10,601.16 hectares (36.45%) to 2,299.86 hectares (7.91%). This is the most significant change in the proportion of landscaping.

**Table 1.** Annotation system for surface coatings in the Hanoi area

| Objects | Sample object in ArcGIS software | Realistic images |
|---|---|---|
| Building land (houses, industrial parks, transportation systems ...) |  |  |
| Water surface (rivers, lakes, ponds) |  |  |
| Plants |  |  |

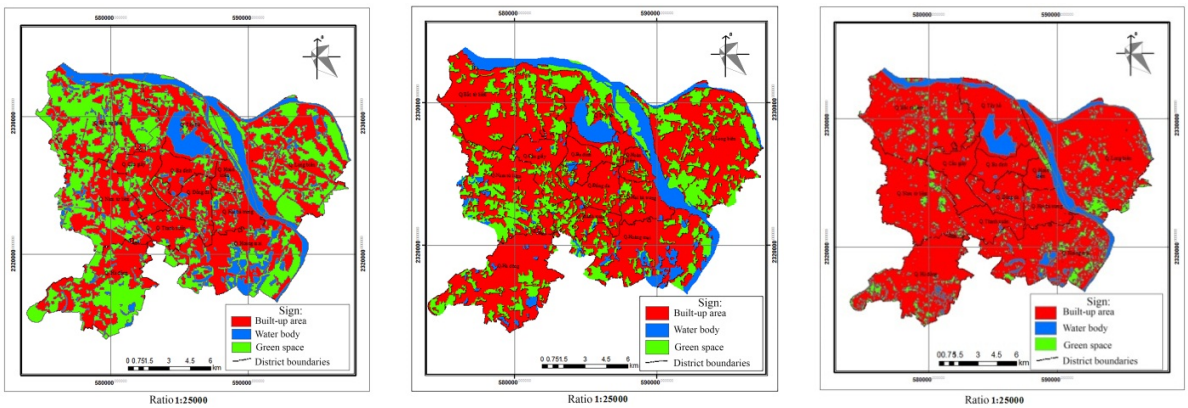


a) b) c)

**Figure 1.** The current state of surface coatings in 12 regions in 2007 (a), 2012 (b), 2017 (c) city [21]

**Table 2.** Area statistics of vegetation types

| No. | Type of land used | 24/05/2007 | | 01/08/2012 | | 04/06/2017 | |
|---|---|---|---|---|---|---|---|
| | | Square (ha) | % | Square (ha) | % | Square (ha) | % |
| **1** | Building land | 14989.56 | 51.53 | 19413.23 | 66.74 | 24705.81 | 84.9 |
| **2** | Water surface | 3497.19 | 12.02 | 3113.93 | 10.71 | 2082.24 | 7.16 |
| **3** | Plants | 10601.16 | 36.45 | 6560.75 | 22.55 | 2299.86 | 7.91 |
| | Total | 29087.91 | 100 | 29087.91 | 100 | 29087.91 | 100 |

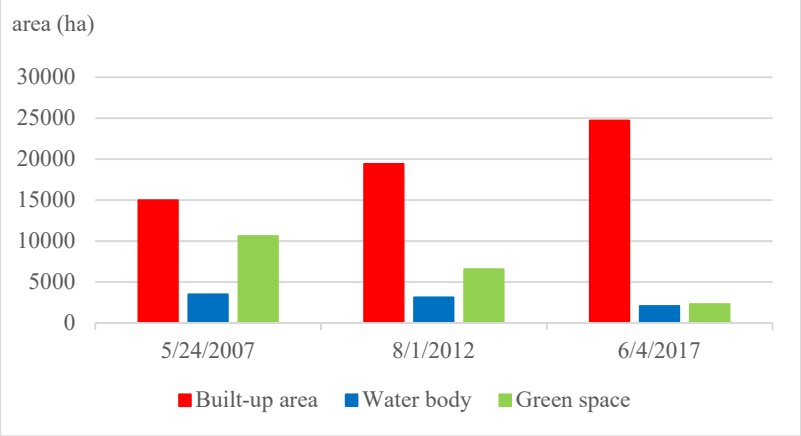


**Figure 2.** Schedule of changes in green areas in urban areas by year. [21] Determination of the true surface temperature in the period 2007, 2012 and 2017

The DN (digital number) value is the value of the pixels stored in digital form. Landsat-5 data is structured as 8 bits; therefore, the enterprise value is from 0 to 28, and Landsat-8 data is structured as 16 bits, therefore the enterprise value is from 0 to 216. The *Lh* value is the energy value, which objects on the soil surface absorb, and then emit into the atmosphere. The process of converting the DN value to the *Lh* value for channels 3, 4 and 6 with Landsat-5 data and channel 10 with Landsat-8 data (table 4) is calculated based on the standard values of emission $L_{MIN\lambda}, L_{MAX\lambda}, Q_{\in AL_{MAX}}, M_L, A_L$ taken from the Metadata file (table 3).

At the final, calculation of the translation value of *Lh* to *TB* must be done. Results in Kelvin units for the thermal infrared channel are shown in table 5.

Determination of surface emission Normalized Difference Vegetation Index (NDVI) is the standardized difference between the reflectivity in the RED and NIR channels. The NDVI index gives us an overall assessment of green plant development, thereby tracking and tracking vegetation changes over time.

Channels RED and NIR - channels 3 and 4 respectively with Landsat-5.7, channels 4 and 5 with Landsat-8. The NDVI index gets a value from -1 to 1, in which the plants are in the range from 0.2 to 1.0. If NDVI > 0.5 - covered vegetation; NDVI < 0.2 - bare soil without vegetation; For water and wet soil, NDVI gets a negative value. The results of the calculation of the NDVI index are shown in table 6. May 24, 2007 is the 114th day in 2007, therefore, the distance d should be taken as the average distance *d* on day 121 and 135. June 4, 2017 is the 155th day of 2017, in which the average distance *d* is per day 121 and 135 is taken as the distance d. The d, $ESUN_h, \theta_{SE}, M_\rho, A_\rho$ values use the calculations shown in table 7, the results calculated by $\rho_\lambda$ are shown in table 8.

**Table 3.** Values $L_{MIN\lambda}, L_{MAX\lambda}, Q_{\in AL_{MAX}}, M_L, A_L$

| | Landsat - 5 | | | Landsat - 7 | | | Landsat - 8 | |
|---|---|---|---|---|---|---|---|---|
| | Channel 3 | Channel 4 | Channel 6 | Channel 3 | Channel 4 | Channel 6.2 | | Channel 10 |
| **Lmax** | 264.000 | 221.000 | 15.303 | 152.900 | 241.100 | 17.040 | Ml | 0.0003342 |
| **Lmin** | -1.170 | -1.510 | 1.238 | -5.000 | -5.100 | 0.000 | Al | 0.1 |
| **Qcal max** | 255.000 | 255.000 | 255.000 | 255.000 | 255.000 | 255.000 | | |

**Table 4.** Values of $L$

| Landsat - 5 (24/5/2007) | | | Landsat - 7 (1/8/2012) | | | Landsat - 8(4/6/2017) |
|---|---|---|---|---|---|---|
| Channel 3 | Channel 4 | Channel 6 | Channel 3 | Channel 4 | Channel 6.2 | Channel 10 |
| $22.47 \le L \le 264$ | $18.65 \le L \le 221$ | $2.506 \le L \le 15.3$ | $26.08 \le L \le 152.9$ | $20.1 \le L \le 194.57$ | $7.25 \le L \le 11.136$ | $8.45 \le L \le 10.658$ |

**Table 5.** Value TB in units K

| Landsat - 5 (Channel 6) | Landsat - 7 (Channel 6.1) | Landsat - 8 (Channel 10) |
|---|---|---|
| 24/5/2007 | 1/8/2012 | 4/6/2017 |
| $295.96 \le TB \le 310.634$ | $296.79 \le TB \le 312.36$ | $296.82 \le TB \le 312.57$ |

Plant Component ($p_v$) is determined by $i, i_v, i_g, p_{2v}, p_{1v}, p_{2g}, p_{1g}$ values for calculating $p_v$, the author conducted a field survey using manual GPS in conjunction with the collected documents along with the image interpretation process. by eye and collecting information from people who have selected 3 typical sampling points, including: a heterogeneous assessment, a uniform assessment of plants, and a uniform point on the ground. The results are shown in table 9.

**Table 6.** Index NDVI

| Landsat - 5 | Landsat - 7 | Landsat - 8 |
|---|---|---|
| 24/5/2007 | 1/8/2012 | 4/6/2017 |
| $-0.383 \le NDVI \le 0.704$ | $-0.57 \le NDVI \le 0.382$ | $-0.142 \le NDVI \le 0.57$ |

**Table 7.** Values d, $ESUN_h, \theta_{SE}, M_\rho, A_\rho$

| | Landsat - 5 (24/5/2007) | | Landsat - 7 (1/8/2012) | | Landsat - 8 (4/6/2017) | |
|---|---|---|---|---|---|---|
| | Channel 3 | Channel 4 | Channel 3 | Channel 4 | | Channel 4,5 |
| **d** | 1.01259 | | 1.0149426 | | $M_\rho$ | 0.00002 |
| $ESUN_h$ | 1.044 | 0.87602 | 0.62165 | 0.96929 | $A_\rho$ | -0.1 |
| $\theta_{SE}$ | 67.3208582 | | 64.84688252 | | $\theta_{SE}$ | 68.41002716 |

**Table 8.** Values $\rho_\lambda$

| Landsat - 5 (24/5/2007) | | Landsat - 7 (1/8/2012) | | Landsat - 8 (4/6/2017) | |
|---|---|---|---|---|---|
| Channel 3 | Channel 4 | Channel 3 | Channel 4 | Channel 4 | Channel 5 |
| $0.03 \le \rho \le 0.33$ | $0.047 \le \rho \le 0.744$ | $0.067 \le \rho \le 0.33$ | $0.251 \le \rho \le 0.92$ | $0.066 \le \rho \le 0.79$ | $0.072 \le \rho \le 1.09$ |

The surface emissivity $\varepsilon$ is evaluated by methods based on the NDVI index are often used to calculate human, if they know the emissivity of bare soil and plants, as well as the distribution structure of plants. Thus, estimating $\varepsilon$ via the RED and NIR channels using the NDVI index will be easier. The values of $\varepsilon_v$ and $\varepsilon_s$ are determined based on the Valor and Caselles correlation plot (1996). Values $\varepsilon_v, \varepsilon_s$ are given in table 10.

**Table 9.** Values $i, i_v, i_g, p_{2v}, p_{1v}, p_{2g}, p_{1g}$ and $p_v$

| Representative point | | Landsat -5 | Landsat - 7 | Landsat - 8 |
|---|---|---|---|---|
| | | 24/5/2007 | 1/8/2012 | 4/6/2017 |
| **Not uniform** | i | 0.296 | 0.148 | 0.292238 |
| **Pure about plants** | $i_v$ | 0.381 | 0.308 | 0.407524 |
| | $p_{2v}$ | 0.264 | 0.826721 | 0.374345 |
| | $p_{1v}$ | 0.036 | 0.087067 | 0.083743 |
| **Purest about the earth** | $i_g$ | 0.118 | 0.106 | 0.124258 |
| | $p_{2g}$ | 0.229 | 0.427294 | 0.304525 |
| | $p_{1g}$ | 0.102 | 0.11477 | 0.209026 |
| **Plant synthesis** | $p_v$ | 0.79 | 0.243 | 0.38253 |

**Table 10.** Values $\varepsilon_v, \varepsilon_s$

| | | Landsat - 5 | Landsat - 8 | |
|---|---|---|---|---|
| | | 24/5/2007 | 1/8/2012 | 4/6/2017 |
| **Diffusing on plant surface** | $\varepsilon_v$ | 0.954 | 0.985 | 0.978 |
| **Diffusing on empty surface** | $\varepsilon_s$ | 0.953 | 0.96 | 0.914 |
| **Surface emission** | $\varepsilon$ | 0.993 | 0.966 | 0.939 |

Calculation of the actual surface temperature with another common method, taking into account the emission factor, often use the average for the whole area. Therefore, the actual surface temperature after the calculation is only relatively accurate. However, using the method of determining $\varepsilon$ by the NDVI index, the actual surface temperature can be estimated quickly, as usual, without complicated computational steps (table 11).

**Table 11.** Value $T_C$ in unit $^{O}C$

| Landsat - 5 | Landsat - 7 | Landsat - 8 |
|---|---|---|
| 24/5/2007 | 1/8/2012 | 4/6/2017 |
| 22.9≤Tc≤37.6 | $23.5 \leq T_C \leq 39.6$ | $24.1 \leq T_C \leq 40.1$ |

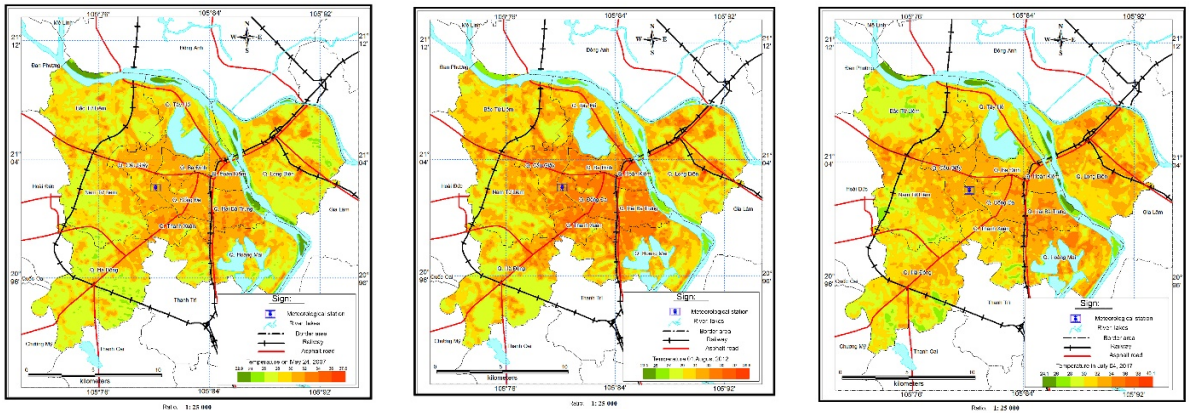

a) b) c)

**Figure 3.** Distributions of surface temperature on May 24, 2007 (a), August 1, 2012 (b) and June 4, 2017

## 4. Conclusion

In general, the results show that land for construction ranks No. 1 in scale and percentage of land cover types from 2007 to 2017. The speed of building land is rapidly increasing in accordance with the context of rapid urbanization in the city of Hanoi. In particular, the share of urban green spaces decreased from 10601.16 hectares (36.45%) to 2299.86 hectares (7.91%) in the period from 2007 to 2017, this is the most significant change in the type of land cover.

Among the most densely populated cities, where the process of urbanization is taking place, the effect of urban heat is created, due to many negative factors for the environment, the life of residents within the municipality, such as: increased energy consumption, increased greenhouse gas emissions into the atmosphere and reduced water quality as well. To resolve the influence of negative processes of a heat island, an urban economy requires a combination of many factors, such as the legal framework of urban planning, design, construction, and building materials. Moreover, to create optimal living and working conditions for urban residents, it is necessary to create sufficient vegetation cover where plants collect moisture through the roots, then keep it in its body (roots and stems), the water is contained on the back of the leaves after. The result is from the liquid state, water turns into vapour and spreads in the air. This natural process is called the transpiration: a kind of natural air conditioning. This natural effect can be observed in hot summer days: walking on the pavement, or asphalt surface and on the grass, there will be a noticeable drop in temperature on the lawn. The use of green roofs for buildings in the city's architecture contributes to the cooling of surfaces, plants also absorb pollutants such as carbon dioxide, and plants, which can reduce the thermal increase on surfaces. Additionally, the use of light surfaces of buildings and planes (roads, sidewalks, platforms) contributes to solving the problem of urban heat island. Mostly, the increase in temperature from an urban city caused by the energy used from fans and air conditioners. Nowadays, the concepts of "green city" and "smart city" are the solution in which the criteria for building a green city have

a great impact on solving the problem as a result of the heat island effect, reducing heat islands in urban areas, reducing emissions, which directly contribute to solve the problem of global warming.

In order for green space to increase the efficiency of urban heat reduction, when planning green space planning, planners should pay more attention to the spatial coverage factor for planning green space for each region towards creating equity in terms of the benefits of heat reduction for all urban residents.

This study revealed the effect of the proportion of scattered green space, the size and shape of green space, with an emphasis on the effect of reducing heat in urban areas of Hanoi. The methodological basis of this work will provide reliable information on the assessment of the thermal state of the city and develop optimal measures to improve the environment in some parts of the city, as well as to describe in detail and predict the formation of the "urban heat island effect".

## References

[1] S. A. Dubrovskaya, and R. Ryakhov, Thermal structures and anomalies of the city of Magnitogorsk based on the results of the interpretation of multispectral images, *Journal: Bulletin of Orenburg State University*, Pp. 286-288, 2015.

[2] I. V. Popova, S. A. Kurolap, and P. M. Vinagradov, Modeling of an urban heat island by means of geoinformation analysis, *Housing and communal infrastructure*, Number 2(5), 2018.

[3] E. A. Baldina, and M. Iu. Gpishenko, Method of decoding multi-temporal space images in the thermal infrared range, *Vestn. Mosk University. Ser. 5. Geography*, vol.3, pp.35-41, 2014.

[4] I. V. Popova, Architectural and climatic analysis of the urban environment (on the example of Voronezh), I. V. Popova, E. V. Sazonov, *Housing and Communal Infrastructure*, № 4 (3), Pp.61-69, 2017.

[5] M. I. Varentsov, P. I. Konstantinov, T. E. Samsonov, and I. A. Repina, Study of the phenomenon of urban heat island in the polar night with the help of experimental measurements and remote sensing on the example of Norilsk, *Modern problems of remote sensing of the Earth from space*, Vol. 11, No. 4, Pp.329–337, 2014.

[6] D. V. Berezin, Reduction of overheating in the local area by rational allocation of green space, D.V. Berezin, *SUSU Bulletin. Series "Construction and Architecture",*V. 13, № 2, Pp. 16-21, 2013.

[7] P. I. Konstantinov, M. Iu. Grishenko, and M. I. Varentsov, Mapping the heat islands of the cities of the Polar region using the combined data of field measurements and satellite images using the example of Apatity (Murmansk region), *EARTH STUDY FROM SPACE*, No. 3, Pp. 27–33, 2015.

[8] M. Iu. Grishenko, and P. I. Konstantinov, The study of the island of heat Moscow 2014-2015, On space and terrestrial data, *an article in the conference proceedings*, Pp. 472-476, 2016.

[9] E. A. Baldina, Study of urban heat islands using remote sensing data in the infrared thermal range / E. A. Baldina, M. Yu. Grishchenko, M. Konstantinov, *Remote sensing in the future Earth, Earth from space "SPECIAL START",* Pp.38-42, 2015.

[10] L. Cui, and Shi, J, Urbanization and its environmental effects in Shanghai, China. Urban Climate, pp.1-15, 2012.

[11] X. X. Li, T. Y. Koh, J. Panda, and L. K. Norford, Impact of urbanization patterns on the local climate of a tropical city, Singapore: An ensemble study. *Journal of Geophysical Research: Atmospheres*, 121(9), pp. 4386-4403, 2016.

[12] T. R. Oke, Urban climates, *Cambridge University Press*, Pp.546, 2017.

[13] Landsat 8 (L8) Data Users Handbook, Version 1.0. June 2015. *Sioux Falls, South Dakota: EROS*, Pp.106, 2015.

[14] D. Kumar, and S. Shekhar, Statistical analysis of land surface temperature–vegetation indexes relationship through thermal remote sensing. *Ecotoxicology and environmental safety*, 121, pp.39-44, 2015.

[15] S. Guha, H. Govil, A. Dey, and N. Gill, Analytical study of land surface temperature with NDVI and NDBI using Landsat 8 OLI and TIRS data in Florence and Naples city, Italy. European *Journal of Remote Sensing*, 51(1), Pp.667-678, 2018.
[16] W. Chen, Y. Zhang, C. Pengwang, and W. Gao, Evaluation of urbanization dynamics and its impacts on surface heat islands: A case study of Beijing, China. *Remote Sensing*, pp 453, 2017.
[17] S. Peng et al. Surface urban heat island across 419 global big cities, *Environ. Sci. & Technol. 2011*, V. 46, № 2, Pp.696–703, 2011.
[18] R. Young-Hee, B. Jong-Jin, Quantitative Analysis of Factors Contributing to Urban Heat Island Intensity, *J. Appl. Meteor. Climatol. 2012*, Vol. 51, Pp. 842–854, 2012.
[19] E. A. Kukanova, P. I. Konstantinov, An urban heat islands climatology in Russia and linkages to the climate change, *Geophysical Research Abstracts of EGU General Assembly*, Vol. 16, pp. 10833, 2014.
[20] M. L. Imhoff, P. Zhang, R. E. Wolfe, and L. Bounoua, Remote sensing of the urban heat island effect across biomes in the continental USA, *Rem. Sens. Environ. 2010*, V. 114, Pp. 504–513,2010.
[21] Minh Tuan Le, Thi Anh Tuyet Cao, Nguyen Anh Quan Tran. The role of green space in the urbanization of Hanoi city, *E3S Web Conf*, Volume 97, N.01013, 2019.